Chapter 19
Particle Swarm Optimisation Aided MIMO Transceiver Designs

S. Chen, W. Yao, H.R. Palally, and L. Hanzo

Abstract. Multiple-input multiple-output (MIMO) technologies are capable of substantially improving the achievable system's capacity, coverage and/or quality of service. The system's ability to approach the MIMO capacity depends heavily on the designs of MIMO receiver and/or transmitter, which are generally expensive optimisation tasks. Hence, researchers and engineers have endeavoured to develop efficient optimisation techniques that can solve practical MIMO designs with affordable costs. In this contribution, we demonstrate that particle swarm optimisation (PSO) offers an efficient means for aiding MIMO transceiver designs. Specifically, we consider PSO-aided semi-blind joint maximum likelihood channel estimation and data detection for MIMO receiver, and we investigate PSO-based minimum bit-error-rate multiuser transmission for MIMO systems. In both these two MIMO applications, the PSO-aided approach attains an optimal design solution with a significantly lower complexity than the existing state-of-the-art scheme.

19.1 Introduction

Multiple-input multiple-output (MIMO) technologies are widely adopted in practice to improve the system's achievable capacity, coverage and/or quality of service [14, 15, 30, 32, 33, 41, 42, 43, 45]. The designs of MIMO receiver and/or transmitter critically influence the system's ability to approach the MIMO capacity. MIMO transceiver designs, which are typically expensive optimisation tasks, have motivated researchers and engineers to develop efficient optimisation techniques that can attain optimal MIMO designs with affordable costs. Hence, the particle swarm optimisation (PSO) as an advanced optimisation tool can offer an efficient means for aiding MIMO transceiver designs. PSO [25] is a population based stochastic optimisation technique inspired by social behaviour of bird flocking or fish schooling. The algorithm commences with random initialisation of a swarm of individuals, referred to as particles, within the problem's search space. It then endeavours to find

S. Chen · W. Yao · H.R. Palally · L. Hanzo
School of Electronics and Computer Science,
University of Southampton, Southampton SO17 1BJ, UK
e-mail: {sqc,wy07r,hrp1v07,lh}@ecs.soton.ac.uk

Y. Tenne and C.-K. Goh (Eds.): Computational Intel. in Expensive Opti. Prob., ALO 2, pp. 487–511.
springerlink.com

a global optimal solution by gradually adjusting the trajectory of each particle toward its own best location and toward the best position of the entire swarm at each evolutionary optimisation step. The PSO method is popular owing to its simplicity in implementation, ability to rapidly converge to a "reasonably good" solution and its robustness against local minima. The PSO method has been successfully applied to wide-ranging optimisation problems [10, 12, 13, 16, 18, 26, 27, 35, 37, 38]. In particular, many research works have applied the PSO techniques to multiuser detection (MUD) [11, 17, 28, 29, 36]. In this contribution we consider the PSO aid MIMO transceiver designs. Specifically, we develop the PSO aided semi-blind joint maximum likelihood (ML) channel estimation and data detection for MIMO receivers and we investigate the PSO-based minimum bit error rate (MBER) multiuser transmission (MUT) for MIMO systems.

In a MIMO receiver, if the channel state information (CSI) is available, optimal ML data detection can be performed using for example the optimised hierarchy reduced search algorithm (OHRSA) aided detector [2], which is an advanced extension of the complex sphere decoder [34]. Accurately estimating a MIMO channel however is a challenging task, and a high proportion of training symbols is required to obtain a reliable least square channel estimate (LSCE) which considerably reduces the achievable system throughput. Although blind joint ML channel estimation and data detection does not reduce the achievable system throughput, it suffers from drawbacks of excessively high computational complexity and an inherent estimation and decision ambiguities [40]. An interesting scheme for semi-blind joint ML channel estimation and data detection has been proposed in [1], in which the joint ML channel estimation and data detection optimisation is decomposed into two levels. At the upper level a population-based optimisation algorithm known as the the repeated weighted boosting search (RWBS) algorithm [7] searches for an optimal channel estimate, while at the lower level the OHRSA detector [2] recovers the transmitted data. Joint ML channel estimation and data detection is achieved by iteratively exchanging information between the RWBS-aided channel estimator and the OHRSA data detector. The scheme is semi-blind as it employs a few training symbols, approximately equal to the rank of the MIMO system, to provide an initial LSCE for aiding the RWBS channel estimator to improve its convergence. The employment of a minimum training overhead has an additional benefit in terms of avoiding the ambiguities inherent in pure blind joint channel estimation and data detection. This study advocates the PSO aided alternative for semi-blind joint ML channel estimation and data detection. We will demonstrate that this PSO aided scheme compares favourably with the existing state-of-the-art RWBS based method, in terms of performance and complexity.

In the downlink of a space-division multiple-access (SDMA) induced MIMO system, mobile terminal (MT) receivers are incapable of cooperatively performing sophisticated MUD. In order to facilitate the employment of a low-complexity high-power efficiency single-user-receiver, the transmitted signals have to be preprocessed at the base station (BS), leading to the appealing concept of multiuser transmission (MUT) [50], provided that accurate downlink CSI is available at the transmitter. The assumption that the downlink channel impulse response (CIR) is

known at the BS may be deemed valid in time division duplex (TDD) systems, where the uplink and downlink signals are transmitted at the same frequency, provided that the co-channel interference is also similar at the BS and the MTs. MUT-aided transmit preprocessing may hence be deemed attractive, when the channel's coherence time is longer than the transmission burst interval. However, for frequency division duplex (FDD) systems, where the uplink and downlink channels are expected to be different, CIR feedback from the MT's receivers to the BS transmitter is necessary [51]. Most of the MUT techniques are designed based on the minimum mean-square-error (MMSE) criterion [44, 51]. Since the achievable bit error rate (BER) is the ultimate system performance indicator, interests on minimum BER (MBER) based MUT techniques have increased recently [21, 39]. The optimal MBER-MUT design is a constrained nonlinear optimisation [21, 39], and the sequential quadratic programming (SQP) algorithm [31] is typically used to obtain the precoder's coefficients for the MBER-MUT [21, 23, 39]. In practice, the computational complexity of the SQP based MBER-MUT solution can be excessive for high-rate systems [23] and, therefore, it is difficult for practical implementation. In this contribution, the PSO algorithm is invoked to find the precoder's coefficients for the MBER-MUT in order to reduce the computational complexity to a practically acceptable level. Our results obtained in [52] have demonstrated that the PSO aided MBER-MUT design imposes a much lower computational complexity than the existing SQP-based MBER-MUT design.

The rest of this contribution is structured as follows. In Section 19.2, the PSO algorithm is presented. Section 19.3 is devoted to the development of the PSO-aided semi-blind joint ML scheme, while Section 19.4 derives the PSO assisted optimal MBER-MUT scheme. Our conclusions are then offered in Section 19.5.

Throughout our discussions we adopt the following notational conventions. Boldface capitals and lower-case letters stand for complex-valued matrices and vectors of appropriate dimensions, respectively, while $\mathbf{I}_K$ and $\mathbf{1}_{K\times L}$ denote the $K\times K$ identity matrix and the $K\times L$ matrix of unity elements, respectively. The (p,q)th element $h_{p,q}$ of $\mathbf{H}$ is also denoted by $\mathbf{H}|_{p,q}$. Furthermore, $(\,)^T$ and $(\,)^H$ represent the transpose and Hermitian operators, respectively, while $\|\,\|^2$ and $|\,|$ denote the norm and the magnitude operators, respectively. $E[\,]$ denotes the expectation operator, while $\Re[\,]$ and $\Im[\,]$ represent the real and imaginary parts, respectively. Finally, $j=\sqrt{-1}$.

19.2 Particle Swarm Optimisation

Consider the generic optimisation task defined as follows

$$\mathbf{U}_{\text{opt}} = \arg\min_{\mathbf{U}} F(\mathbf{U}) \tag{19.1}$$

$$\text{s.t. } \mathbf{U}\in\mathsf{U}^{N\times M} \tag{19.2}$$

where $F(\,)$ is the cost function of the optimisation problem, $\mathbf{U}$ is a $N\times M$ complex-valued parameter matrix to be optimised, and

$$\mathsf{U} = \left[-U_{\max},\, U_{\max}\right] + j\left[-U_{\max},\, U_{\max}\right] \tag{19.3}$$

defines the search range for each element of $\mathbf{U}$. The flowchart of the PSO algorithm is given in Fig. 19.1. A swarm of particles, $\{\mathbf{U}_i^{(l)}\}_{i=1}^{S}$, that represent potential solutions are evolved in the search space $\mathsf{U}^{N\times M}$, where S is the swarm size and index l denotes the iteration step. The details of the algorithm is now explained.

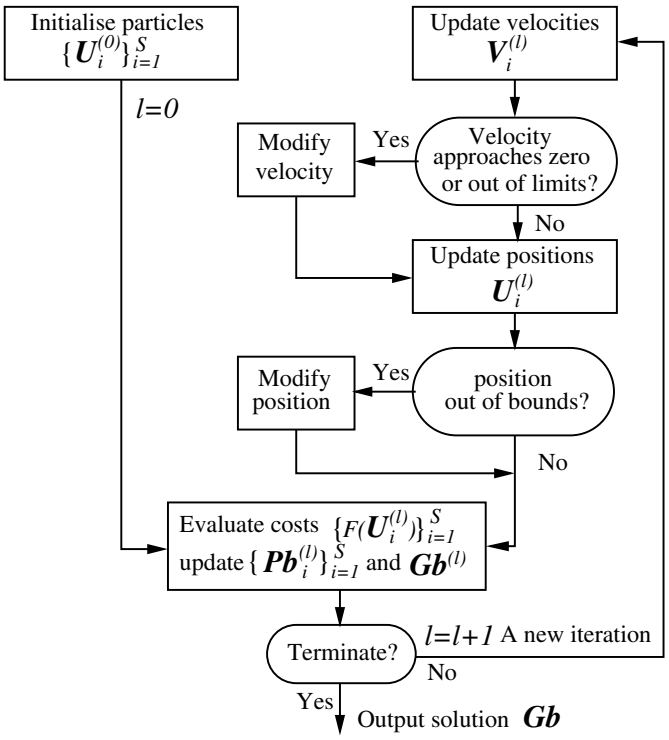

Fig. 19.1 Flowchart of the PSO algorithm

19.2.1 PSO Algorithm

a) The swarm initialisation. Set $l = 0$ and generate the initial particles, $\{\mathbf{U}_i^{(l)}\}_{i=1}^{S}$, in the search space $\mathsf{U}^{N\times M}$ with a prescribed way. Typically, the initial particles are randomly generated.

b) The swarm evaluation. For each particle $\mathbf{U}_i^{(l)}$, compute its associated cost $F\left(\mathbf{U}_i^{(l)}\right)$. Each particle $\mathbf{U}_i^{(l)}$ remembers its best position visited so far, denoted as $\mathbf{Pb}_i^{(l)}$, which provides the cognitive information. Every particle also knows the best position visited so far among the entire swarm, denoted as $\mathbf{Gb}^{(l)}$, which provides the social

information. The cognitive information $\{\mathbf{Pb}_i^{(l)}\}_{i=1}^{S}$ and the social information $\mathbf{Gb}^{(l)}$ are updated at each iteration:

For $(i = 1; i \leq S; i{+}{+})$
  If $(F(\mathbf{U}_i^{(l)}) < F(\mathbf{Pb}_i^{(l)}))$ $\mathbf{Pb}_i^{(l)} = \mathbf{U}_i^{(l)}$;
End for;
$i^* = \arg\min_{1\leq i\leq S} F(\mathbf{Pb}_i^{(l)})$;
If $(F(\mathbf{Pb}_{i^*}^{(l)}) < F(\mathbf{Gb}^{(l)}))$ $\mathbf{Gb}^{(l)} = \mathbf{Pb}_{i^*}^{(l)}$;

c) The swarm update. Each particle $\mathbf{U}_i^{(l)}$ has a velocity, denoted as $\mathbf{V}_i^{(l)}$, to direct its "flying" or search within the search space. The velocity and position of the ith particle are updated in each iteration according to:

$$\mathbf{V}_i^{(l+1)} = \xi * \mathbf{V}_i^{(l)} + c_1 * \varphi_1 * (\mathbf{Pb}_i^{(l)} - \mathbf{U}_i^{(l)}) + c_2 * \varphi_2 * (\mathbf{Gb}^{(l)} - \mathbf{U}_i^{(l)}), \quad (19.4)$$

$$\mathbf{U}_i^{(l+1)} = \mathbf{U}_i^{(l)} + \mathbf{V}_i^{(l+1)}, \quad (19.5)$$

where ξ is the inertia weight, c_1 and c_2 are the two empirically chosen acceleration coefficients, while $\varphi_1 = rand()$ and $\varphi_2 = rand()$ denotes the two random variables uniformly distributed in $(0,\ 1)$.

In order to avoid excessive roaming of particles beyond the search space [18], a velocity space $\mathsf{V}^{N\times M}$ with

$$\mathsf{V} = \left[-V_{\max},\ V_{\max}\right] + j\left[-V_{\max},\ V_{\max}\right] \quad (19.6)$$

is imposed so that each element of $\mathbf{V}_i^{(l+1)}$ is within the search range V defined in (19.6), namely,

If $(\Re[\mathbf{V}_i^{(l+1)}|_{p,q}] > V_{\max})$ $\Re[\mathbf{V}_i^{(l+1)}|_{p,q}] = V_{\max}$;
If $(\Re[\mathbf{V}_i^{(l+1)}|_{p,q}] < -V_{\max})$ $\Re[\mathbf{V}_i^{(l+1)}|_{p,q}] = -V_{\max}$;
If $(\Im[\mathbf{V}_i^{(l+1)}|_{p,q}] > V_{\max})$ $\Im[\mathbf{V}_i^{(l+1)}|_{p,q}] = V_{\max}$;
If $(\Im[\mathbf{V}_i^{(l+1)}|_{p,q}] < -V_{\max})$ $\Im[\mathbf{V}_i^{(l+1)}|_{p,q}] = -V_{\max}$;

Moreover, if $\mathbf{V}_i^{(l+1)}$ approaches zero, it is reinitialised proportional to $V_{\max}$ with a small control factor γ according to:

If $(\Re[\mathbf{V}_i^{(l+1)}|_{p,q}] == 0)$
  If$(rand() < 0.5)$
    $\Re[\mathbf{V}_i^{(l+1)}|_{p,q}] = \varphi_v * \gamma * V_{\max}$;
  Else
    $\Re[\mathbf{V}_i^{(l+1)}|_{p,q}] = -\varphi_v * \gamma * V_{\max})$;
  End if;
Else if $(\Im[\mathbf{V}_i^{(l+1)}|_{p,q}] == 0)$
  If$(rand() < 0.5)$
    $\Im[\mathbf{V}_i^{(l+1)}|_{p,q}] = \varphi_v * \gamma * V_{\max}$;

Else
$\Im[\mathbf{V}_i^{(l+1)}|_{p,q}] = -\varphi_v * \gamma * V_{\max})$;
End if;
End if;

where $\varphi_v = rand()$ is another uniform random variable in $(0,\ 1)$.

Similarly, each $\mathbf{U}_i^{(l+1)}$ is checked to ensure that it stays inside the search space $\mathsf{U}^{N\times M}$. This can be done for example with the rule:

If $(\Re[\mathbf{U}_i^{(l+1)}|_{p,q}] > U_{\max})$ $\Re[\mathbf{U}_i^{(l+1)}|_{p,q}] = U_{\max}$;
If $(\Re[\mathbf{U}_i^{(l+1)}|_{p,q}] < -U_{\max})$ $\Re[\mathbf{U}_i^{(l+1)}|_{p,q}] = -U_{\max}$;
If $(\Im[\mathbf{U}_i^{(l+1)}|_{p,q}] > U_{\max})$ $\Im[\mathbf{U}_i^{(l+1)}|_{p,q}] = U_{\max}$;
If $(\Im[\mathbf{U}_i^{(l+1)}|_{p,q}] < -U_{\max})$ $\Im[\mathbf{U}_i^{(l+1)}|_{p,q}] = -U_{\max}$;

An alternative rule is, if a particle is outside the search space, it is moved back inside the search space randomly, rather than forcing it to stay at the border as the previous rule does. That is,

If $(\Re[\mathbf{U}_i^{(l+1)}|_{p,q}] > U_{\max})$ $\Re[\mathbf{U}_i^{(l+1)}|_{p,q}] = rand() * U_{\max}$;
If $(\Re[\mathbf{U}_i^{(l+1)}|_{p,q}] < -U_{\max})$ $\Re[\mathbf{U}_i^{(l+1)}|_{p,q}] = -rand() * U_{\max}$;
If $(\Im[\mathbf{U}_i^{(l+1)}|_{p,q}] > U_{\max})$ $\Im[\mathbf{U}_i^{(l+1)}|_{p,q}] = rand() * U_{\max}$;
If $(\Im[\mathbf{U}_i^{(l+1)}|_{p,q}] < -U_{\max})$ $\Im[\mathbf{U}_i^{(l+1)}|_{p,q}] = -rand() * U_{\max}$;

This is similar to the checking procedure given in [18].

d) Termination condition check. If the maximum number of iterations, $I_{\max}$, is reached, terminate the algorithm with the solution $\mathbf{U}_{\text{opt}} = \mathbf{G}\mathbf{b}^{(I_{\max})}$; otherwise, set $l = l + 1$ and go to Step *b)*.

19.2.2 Complexity of PSO Algorithm

Let the computational complexity of one cost function evaluation be C_{single}. Given the swarm size S, assume that the algorithm converges in $I_{\max}$ iterations. Then the total number of cost function evaluations is simply $N_{\text{total}} = S \times I_{\max}$, and the complexity of the algorithm is given by

$$C = N_{\text{total}} \times C_{\text{single}} = S \times I_{\max} \times C_{\text{single}}. \tag{19.7}$$

19.2.3 Choice of PSO Algorithmic Parameters

We now comment on the choices of PSO algorithmic parameters. The search bound $U_{\max}$ is specified by the optimisation problem considered, while the velocity limit $V_{\max}$ is typically related to the value of $U_{\max}$. The swarm size S depends on how hard the optimisation problem (19.1) is. For small to medium size optimisation problems, a standard choice recommended in the literature is $S = 20$ to 50. The maximum

number of iterations, $I_{\max}$, is generally determined by experiment. In our experiments we choose the optimal swarm size S to minimise the total complexity C of (19.7).

It was reported in [35] that a time varying acceleration coefficient (TVAC) enhances the performance of PSO. In this TVAC mechanism [35], c_1 for the cognitive component is reduced from 2.5 to 0.5 and c_2 for the social component varies from 0.5 to 2.5 respectively during the iterative procedure according to

$$\left.\begin{aligned} c_1 &= (0.5-2.5)*l/I_{\max}+2.5 \\ c_2 &= (2.5-0.5)*l/I_{\max}+0.5 \end{aligned}\right\} \tag{19.8}$$

The reason given for this TVAC mechanism is that at the initial stages, a large cognitive component and a small social component help particles to wander around or exploit better the search space and to avoid local minima. In the later stages, a small cognitive component and a large social component help particles to converge quickly to a global minimum.

We also experiment an alternative TVAC mechanism in which c_1 is varies from 0.5 to 2.5 and c_2 changes from 2.5 to 0.5 during the iterative procedure according to

$$\left.\begin{aligned} c_1 &= (2.5-0.5)*l/I_{\max}+0.5 \\ c_2 &= (0.5-2.5)*l/I_{\max}+2.5 \end{aligned}\right\} \tag{19.9}$$

Which TVAC mechanism to choose is decided by empirical performance in our applications.

Several choices of the inertia weight can be considered, including the zero inertia weight $\xi = 0$, a constant inertia weight ξ or a random inertia weight $\xi = rand()$. In our applications, empirical experience suggests that $\xi = 0$ is appropriate. An appropriate value of the control factor γ in reinitialising zero velocity found empirically for our applications is $\gamma = 0.1$.

19.3 PSO Aided Semi-blind Joint ML Estimation

Our first application of PSO to multiple-input multiple-output (MIMO) transceiver design involves the PSO-aided semi-blind joint maximum likelihood (ML) channel estimation and data detection for MIMO receiver.

19.3.1 MIMO System Model

We consider a MIMO system consisting of n_T transmitters and n_R receivers, which communicates over flat fading channels [42]. The system is described by the well-known MIMO model [32]

$$\mathbf{y}(k) = \mathbf{H}\mathbf{x}(k) + \mathbf{n}(k), \tag{19.10}$$

where k is the symbol index, $\mathbf{H}$ denotes the $n_R \times n_T$ complex-valued MIMO channel matrix, $\mathbf{x}(k) = [x_1(k)\ x_2(k) \cdots x_{n_T}(k)]^T$ is the transmitted symbols vector of the n_T transmitters with the symbol energy given by $E\left[|x_m(k)|^2\right] = \sigma_x^2$ for $1 \le m \le n_T$, $\mathbf{y}(k) = [y_1(k)\ y_2(k) \cdots y_{n_R}(k)]^T$ denotes the received signal vector, and $\mathbf{n}(k) = [n_1(k)\ n_2(k) \cdots n_{n_R}(k)]^T$ is the complex-valued Gaussian white noise vector associated with the MIMO channels with $E\left[\mathbf{n}(k)\mathbf{n}^H(k)\right] = 2\sigma_n^2 \mathbf{I}_{n_R} = \mathrm{N_o}\mathbf{I}_{n_R}$. The signal-to-noise ratio (SNR) of the system is defined by $\mathrm{SNR} = \mathrm{E_b}/\mathrm{N_o} = \sigma_x^2/2\sigma_n^2$.

More specifically, the narrowband MIMO channel matrix is defined by $\mathbf{H} = [h_{p,m}]$, for $1 \le p \le n_R$ and $1 \le m \le n_T$, where $h_{p,m}$ denotes the channel coefficient linking the mth transmitter to the pth receiver. The fading is assumed to be sufficiently slow, so that during the time period of a short block of L symbols, all the entries in the MIMO channel matrix $\mathbf{H}$ may be deemed unchanged. From frame to frame, the channel impulse response (CIR) taps $h_{p,m}$ are independently and identically distributed (i.i.d.) complex-valued Gaussian processes with zero mean and $E\left[|h_{p,m}|^2\right] = 1$. Note that frequency selective MIMO channels can be made narrowband using for example the orthogonal frequency division multiplexing (OFDM) technique [19]. We also assume that the modulation scheme is the quadrature phase shift keying (QPSK) and, therefore, the transmitted symbol takes the value from the symbol set

$$x_i(k) \in \mathscr{X} = \{\pm 1 \pm j\}. \tag{19.11}$$

All the results discussed here are equally applicable to higher-throughput modulation schemes, such as the quadrature amplitude modulation (QAM) [20], with increased complexity.

19.3.2 Semi-blind Joint ML Channel Estimation and Data Detection

Let us consider the joint channel estimation and data detection based on the observation vector $\mathbf{y}(k)$ over a relatively short length of L symbols. First define the $n_R \times L$ matrix of the received data as $\mathbf{Y} = [\mathbf{y}(1)\ \mathbf{y}(2) \cdots \mathbf{y}(L)]$ and the corresponding $n_T \times L$ matrix of the transmitted symbols as $\mathbf{X} = [\mathbf{x}(1)\ \mathbf{x}(2) \cdots \mathbf{x}(L)]$. Then the probability density function (PDF) of the received data matrix $\mathbf{Y}$ conditioned on the MIMO channel matrix $\mathbf{H}$ and the transmitted symbol matrix $\mathbf{X}$ can be written as

$$p(\mathbf{Y}|\mathbf{H},\mathbf{X}) = \frac{1}{(2\pi\sigma_n^2)^{n_R \times L}} e^{-\frac{1}{2\sigma_n^2}\sum_{k=1}^{L}\|\mathbf{y}(k)-\mathbf{H}\mathbf{x}(k)\|^2}. \tag{19.12}$$

The ML estimation of $\mathbf{X}$ and $\mathbf{H}$ can be obtained by jointly maximising $p(\mathbf{Y}|\mathbf{H},\mathbf{X})$ over $\mathbf{X}$ and $\mathbf{H}$. Equivalently, the joint ML estimation is obtained by minimsing the cost function

$$J_{\mathrm{ML}}(\check{\mathbf{X}},\check{\mathbf{H}}) = \frac{1}{n_R \times L}\sum_{k=1}^{L}\left\|\mathbf{y}(k) - \check{\mathbf{H}}\,\check{\mathbf{x}}(k)\right\|^2, \tag{19.13}$$

which is a function of the symbol matrix $\check{\mathbf{X}} = [\check{\mathbf{x}}(1)\ \check{\mathbf{x}}(2)\cdots\check{\mathbf{x}}(L)]$ and the channel matrix $\check{\mathbf{H}}$. Thus the joint ML channel and data estimation is obtained as

$$(\hat{\mathbf{X}}, \hat{\mathbf{H}}) = \arg\left\{\min_{\check{\mathbf{X}},\check{\mathbf{H}}} J_{\mathrm{ML}}(\check{\mathbf{X}}, \check{\mathbf{H}})\right\}. \tag{19.14}$$

The joint ML optimisation defined in (19.14) is computationally prohibitive. The complexity of this optimisation process may be reduced to a tractable level, if it is decomposed into an iterative search carried out over all the possible data symbols first and then over the channel matrices as

$$(\hat{\mathbf{X}}, \hat{\mathbf{H}}) = \arg\left\{\min_{\check{\mathbf{H}}}\left[\min_{\check{\mathbf{X}}} J_{\mathrm{ML}}(\check{\mathbf{X}}, \check{\mathbf{H}})\right]\right\}. \tag{19.15}$$

At the inner-level optimisation we can use the the optimised hierarchy reduced search algorithm (OHRSA) based ML detector [2] to find the ML data estimate for the given channel. The detailed implementation of the OHRSA-aided ML detector can be found in [2] and will not be repeated here. In order to guarantee a joint ML estimate, the search algorithm used at the outer or upper-level optimisation should be capable of finding a global optimal channel estimate efficiently. A joint ML solution is achieved with the following iterative loop.

Outer-level Optimisation: A search algorithm searches the MIMO channel parameter space to find a global optimal estimate $\hat{\mathbf{H}}$ by minimising the mean square error (MSE)

$$J_{\mathrm{MSE}}(\check{\mathbf{H}}) = J_{\mathrm{ML}}(\hat{\mathbf{X}}(\check{\mathbf{H}}), \check{\mathbf{H}}), \tag{19.16}$$

where $\hat{\mathbf{X}}(\check{\mathbf{H}})$ denotes the ML estimate of the transmitted data for the given channel $\check{\mathbf{H}}$.

Inner-level Optimisation: Given $\check{\mathbf{H}}$ the OHRSA detector finds the ML estimate of the transmitted data and feeds back the ML metric $J_{\mathrm{MSE}}(\check{\mathbf{H}})$ to the upper level.

Pure blind joint data and channel estimation converges very slowly and suffers from an inherent permutation and scaling ambiguity problem [40]. To resolve this permutation and scaling ambiguity, a few training symbols are employed to provide an initial least square channel estimate (LSCE) for aiding the outer-level search algorithm. Let the number of training symbols be K, and denote the available training data as $\mathbf{Y}_K = [\mathbf{y}(1)\ \mathbf{y}(2)\cdots\mathbf{y}(K)]$ and $\mathbf{X}_K = [\mathbf{x}(1)\ \mathbf{x}(2)\cdots\mathbf{x}(K)]$. The LSCE based on $\{\mathbf{Y}_K, \mathbf{X}_K\}$ is readily given by

$$\check{\mathbf{H}}_{\mathrm{LSCE}} = \mathbf{Y}_K \mathbf{X}_K^H \left(\mathbf{X}_K \mathbf{X}_K^H\right)^{-1}. \tag{19.17}$$

To maintain the system throughput, we only use the minimum number of training symbols, namely, $K = n_T$, which is equal to the rank of the MIMO system. The training symbol matrix $\mathbf{X}_K$ should be designed to yield the optimal estimation performance [4]. Specifically, $\mathbf{X}_K$ is designed to have n_T orthogonal rows. This yields the most efficient estimate and removes the need for matrix inversion.

19.3.3 PSO Aided Semi-blind Joint ML Scheme

The above semi-blind joint ML data and channel estimation is a very expensive optimisation problem. Firstly, let us exam the inner-level optimisation. For a given channel $\check{\mathbf{H}}$, the ML data detection solution $\hat{\mathbf{X}}(\check{\mathbf{H}})$ must be calculated. Note that the data matrix $\check{\mathbf{X}}$ has $\mathscr{M}^{L\times n_R}$ legitimate combinations, where $\mathscr{M}=4$ is the size of the QPSK symbol set (19.11). A exhausted search would require to calculate the cost function (19.13) $\mathscr{M}^{L\times n_R}$ times and to find the data matrix that attains the minimum value of the cost function. This is obviously prohibitive. The OHRSA-aided ML detector [2] manages to reduce dramatically the complexity required for attainding the ML solution $\hat{\mathbf{X}}(\check{\mathbf{H}})$. Even so the OHRSA detector is by no means low-complexity and is in fact inherently expensive owing to the nature of the optimal ML detection. The detailed complexity analysis can be found for example in [46] and is beyond the scope of this contribution. Now consider the outer-level optimisation, which has to search through the $(2n_R)\times(2n_T)$ dimensional real-valued channel space. Each point evaluated requires to call the OHRSA detector once. Any search algorithm will require a large number of OHRSA evaluations in order to attain the joint ML solution $\hat{\mathbf{X}}(\hat{\mathbf{H}})$.

In the previous work [1], we have applied the repeated weighted boosting search (RWBS) algorithm [7] to perform the outer-level optimisation search of the joint ML iterative loop. The results shown in [1] demonestrate that the RWBS-aided semi-blind joint ML scheme performs well and is efficient in terms of its convergence speed. In this contribution, we show that by invoking the PSO method as the outer-level search algorithm, further performance enhancement can be achieved in terms of reduced complexity. The cost function for the PSO algorithm to optimise in this case is $F(\check{\mathbf{H}})=J_{\rm MSE}(\check{\mathbf{H}})$ with the dimensions of the search space specified by $N=n_R$ and $M=n_T$.

In Step *a) The swarm initialisation*, the initial particles are chosen as $\check{\mathbf{H}}_1^{(0)}=\check{\mathbf{H}}_{\rm LSCE}$ and

$$\check{\mathbf{H}}_i^{(0)}=\check{\mathbf{H}}_{\rm LSCE}+\varphi_h(\mathbf{1}_{n_R\times n_T}+j\mathbf{1}_{n_R\times n_T}),\ 2\le i\le S, \tag{19.18}$$

where φ_h is a uniformly distributed random variable defined in the range $[-\alpha,\ \alpha]$. Appropriate value for α is determined by experiment.

In Step *c) The swarm update*, we adopt the zero inertia weight $\xi=0$ and the TVAC mechanism (19.9). For any particle wandering outside the search space, we force it back to stay at the border of the search space. These provisions are found to be appropriate for this application empirically.

Let $C_{\rm OHRSA}(L)$ be the complexity of the OHRSA algorithm to decode the L-symbol data matrix $\mathbf{X}$ and let $N_{\rm OHRSA}$ be the number of calls for the OHRSA algorithm required by the PSO algorithm to converge. Then the complexity of the proposed semi-blind method is expressed as

$$C=N_{\rm OHRSA}\times C_{\rm OHRSA}(L), \tag{19.19}$$

where $C_{\rm OHRSA}(L)$ is given in [46], and $N_{\rm OHRSA}=S\times I_{\max}$ with $I_{\max}$ being the maximum number of iterations and S the swarm size. It can be seen that the

computational complexity of the PSO aided semi-blind joint ML estimation scheme is characterised by the number of OHRSA cost function evaluations N_{OHRSA}. Obviously, the number of iterations that the PSO algorithm requires to converge is $I_{\max}$, and the value of $I_{\max}$ depends on the choice of S. It is easily seen that the optimal choice of the swarm size S should lead to the minimum value of N_{OHRSA}.

19.3.4 Simulation Study

A simulation study was carried out to investigate the PSO aided semi-blind joint ML channel estimation and data detection scheme. We considered the benchmark MIMO system with $n_T = 4$ and $n_R = 4$ used in [1]. The achievable performance was assessed in the simulation using three metrics, and these were the MSE defined in (19.16), the mean channel error (MCE) defined as

$$J_{\text{MCE}}(\check{\mathbf{H}}) = \|\mathbf{H} - \check{\mathbf{H}}\|^2, \tag{19.20}$$

where $\mathbf{H}$ denotes the true MIMO channel matrix and $\check{\mathbf{H}}$ the channel estimate, and the bit error rate (BER). All the simulation results were averaged over 50 different channel realisations of $\mathbf{H}$.

We set the population size to $S = 20$, which led to the maximum number of evolutionary steps $I_{\max} = 50$. This choice of S appeared to be adequate for this application as it resulted in the smallest N_{OHRSA} for the algorithm to converge. Thus, the complexity of the PSO based semi-blind scheme was determined by $N_{\text{OHRSA}} = 1000$. Since $\Re[h_{p,q}]$ and $\Im[h_{p,q}]$ of each MIMO channel tap $h_{p,q}$ were Gaussian distributed with a variance 0.5, we chose the search space bound to be $U_{\max} = 1.8$

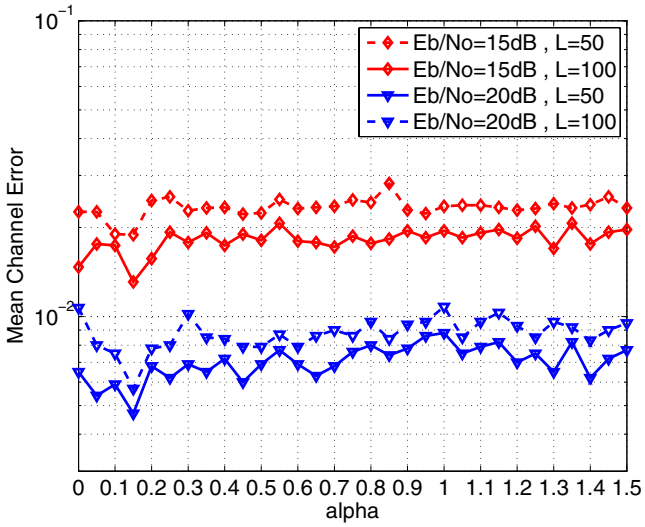

Fig. 19.2 Mean channel error average over 50 different channel realisations as a function of α after 1000 OHRSA evaluations, for two values of $\mathrm{E_b/N_o}$ and two values of L

which lay between 2 to 3 standard deviations of the true tap distribution. We also set the velocity limit to $V_{\max} = 1.0$ which was confirmed in simulation to be a suitable value for this application. The control factor γ in reinitialising zero velocity was found empirically to be $\gamma = 0.1$. The optimal value for the control parameter α in the channel population initiation (19.18) was first found empirically. Fig. 19.2 shows the MCE performance after 1000 OHRSA evaluations over a range of α values. It can be seen from Fig. 19.2 that the optimal value of α in this case was 0.15. This value of α was used in all the other simulations.

Fig. 19.3 depicts the BER performance of the PSO based semi-blind scheme having a frame length $L = 100$ after 1000 OHRSA evaluations and averaging over 50 different channel realisations, in comparison with the performance of the training-based OHRSA detector having $K = 4$, 8 and 16 training symbols for the LSCE, respectively, as well as with the case of perfect channel knowledge. It can be observed from Fig. 19.3 that, for the training-based scheme to achieve the same BER performance of the PSO-aided semi-blind one having only 4 pilot symbols, the number of training symbols had to be more than 16. This example was identical to the MIMO system investigated in [1]. The BER performance of the PSO-based semi-blind scheme depicted in Fig. 19.3 was slightly better than the BER of the RWBS-based semi-blind scheme shown in [1]. Moreover, the performance of the PSO-aided scheme was achieved after 1000 OHRSA evaluations, while the performance of the RWBS-based scheme reported in [1] was obtained after 1200 OHRSA evaluations. Thus, for this 4×4 MIMO benchmark, the computational saving achieved by the

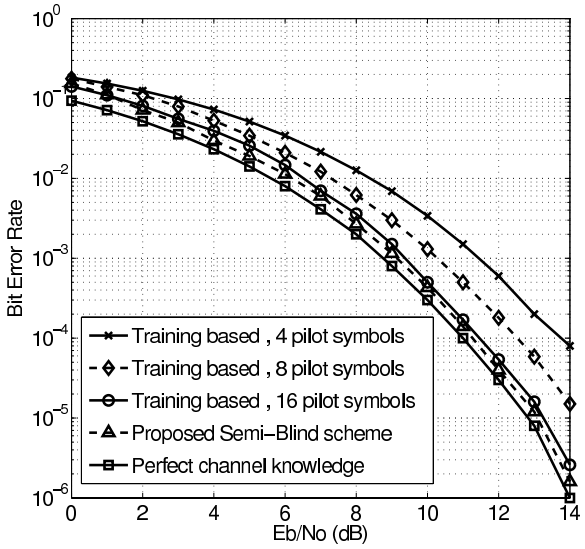

Fig. 19.3 BER of the PSO aided semi-blind scheme with frame length $L = 100$ after 1000 OHRSA evaluations and average over 50 different channel realisations in comparison with the training-based cases using 4, 8 and 16 pilot symbols as well as the case of perfect channel knowledge

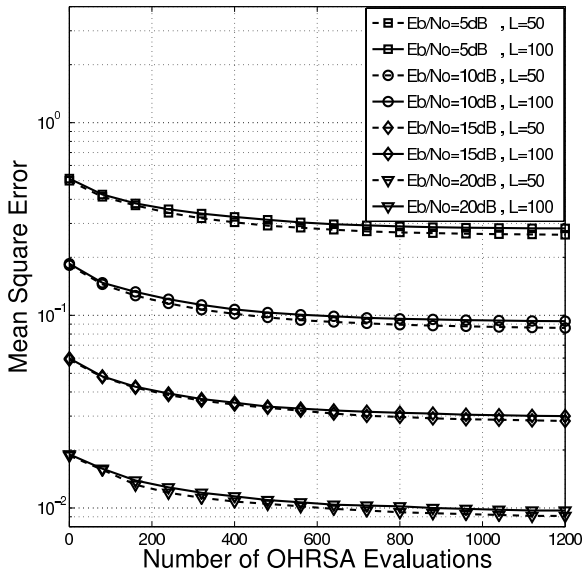

Fig. 19.4 Mean square error convergence performance of the PSO aided semi-blind scheme averaged over 50 different channel realisations for different values of E_b/N_o and L

proposed PSO-based semi-blind method over the previous RWBS-based scheme was approximately

$$\frac{1200 \times C_{\text{OHRSA}}(L) - 1000 \times C_{\text{OHRSA}}(L)}{1000 \times C_{\text{OHRSA}}(L)} = 20\%. \tag{19.21}$$

Figs. 19.4 and 19.5 depict the convergence performance of the proposed PSO-aided semi-blind joint ML channel estimation and data detection scheme averaged over 50 different channel realisations in terms of the MSE and MCE, respectively, for different SNR values as well as for two frame lengths $L = 50$ and 100. It can be seen from Fig. 19.4 that the MSE converged to the noise floor. The MCE performance shown in Fig. 19.5 was seen to be slightly better and converging faster than the results obtained by the RWBS-based semi-blind joint ML scheme shown in [1].

19.4 PSO Based MBER Multiuser Transmitter Design

In this second application, we adopt the PSO for designing the minimum BER (MBER) multiuser transmission (MUT) for the downlink of a space-division multiple-access (SDMA) induced MIMO system.

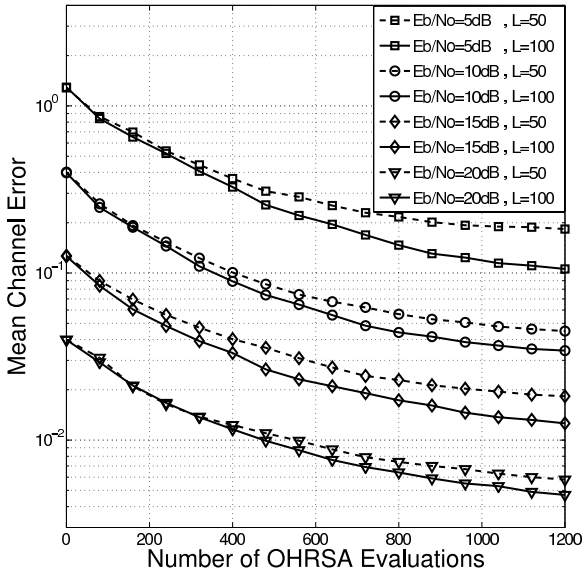

Fig. 19.5 Mean channel error convergence performance of the PSO aided semi-blind scheme averaged over 50 different channel realisations for different values of E_b/N_o and L

19.4.1 Downlink of SDMA Induced MIMO System

In the downlink of the SDMA induced MIMO system, the base station (BS) equipped with n_T transmit antennas communicates over flat fading channels with n_R mobile terminals (MTs), each employing a single-receive antenna. Again we point out that frequency selective channels can be converted to a multiplicity of parallel narrowband channels using the OFDM technique [19]. Let the vector of n_R information symbols transmitted in the downlink be $\mathbf{x}(k) = [x_1(k)\ x_2(k) \cdots x_{n_R}(k)]^T$, where k denotes the symbol index, $x_m(k)$ denotes the transmitted symbol to the mth MT, and the symbol energy is given by $E[|x_m(k)|^2] = \sigma_x^2$, for $1 \le m \le n_R$. The modulation scheme is again assumed to be the QPSK of the symbol set (19.11), but the extension to the generic QAM modulation scheme can be achieved by considering the minimum symbol error rate criterion [9]. The $n_T \times n_R$ precoder matrix $\mathbf{C}$ of the BS's MUT is defined by

$$\mathbf{C} = [\mathbf{c}_1\ \mathbf{c}_2 \cdots \mathbf{c}_{n_R}], \tag{19.22}$$

where $\mathbf{c}_m$, $1 \le m \le n_R$, is the precoder's coefficient vector for pre-processing the mth user's data stream. Given a fixed total transmit power E_T at the BS, an appropriate scaling factor should be used to fullfill this transmit power constraint, which is defined as

$$\rho = \sqrt{E_T / E[\|\mathbf{C}\mathbf{x}(k)\|^2]}. \tag{19.23}$$

Thus, the signal vector to be launched from the n_T transmit antennas is $\rho\mathbf{C}\mathbf{x}(k)$.

The downlink of the SDMA system is specified by its channel matrix $\mathbf{H}$, which is given by

$$\mathbf{H} = [\mathbf{h}_1\ \mathbf{h}_2 \cdots \mathbf{h}_{n_R}], \tag{19.24}$$

where $\mathbf{h}_m = [h_{1,m}\ h_{2,m} \cdots h_{n_T,m}]^T$, $1 \le m \le n_R$, is the mth user's spatial signature. The channel taps $h_{i,m}$ for $1 \le i \le n_T$ and $1 \le m \le n_R$ are independent of each other and obey the complex-valued Gaussian distribution with $E[|h_{i,m}|^2] = 1$. At the receiver, the reciprocal of the scaling factor, namely ρ^{-1}, is used to scale the received signal to ensure unity-gain transmission, and the baseband model of the system can be described as

$$\mathbf{y}(k) = \rho^{-1}\mathbf{H}^T \rho\, \mathbf{C}\,\mathbf{x}(k) + \rho^{-1}\mathbf{n}(k) = \mathbf{H}^T \mathbf{C}\,\mathbf{x}(k) + \rho^{-1}\mathbf{n}(k), \tag{19.25}$$

where $\mathbf{n}(k) = [n_1(k)\ n_2(k) \cdots n_{n_R}(k)]^T$ is the channel additive white Gaussian noise vector, $n_m(k)$, $1 \le m \le n_R$, is a complex-valued Gaussian random process with zero mean and $E[|n_m(k)|^2] = 2\sigma_n^2 = \mathrm{N_o}$, and $\mathbf{y}(k) = [y_1(k)\ y_2(k) \cdots y_{n_R}(k)]^T$ denotes the received signal vector. Note that $y_m(k)$, $1 \le m \le n_R$, constitutes sufficient statistics for the mth MT to detect the transmitted data symbol $x_m(k)$. The SNR of the downlink is defined as $\mathrm{SNR} = \mathrm{E_b}/\mathrm{N_o}$, where $\mathrm{E_b} = \mathrm{E_T}/(n_T \log_2 \mathscr{M})$ is the energy per bit per antenna for $\mathscr{M}$-ary modulation. In our case, $\mathscr{M} = 4$.

19.4.2 MBER MUT Design

The minimum mean square error (MMSE) MUT design, denoted as $\mathbf{C}_{\mathrm{TxMMSE}}$, is popular owing to its appealing simplicity [44, 51], but it does not minimise the achievable system's BER. The average BER of the in-phase component of $\mathbf{y}(k)$ at the receiver is given by [8]

$$P_{e_I}(\mathbf{C}) = \frac{1}{n_R \mathscr{M}^{n_R}} \sum_{q=1}^{\mathscr{M}^{n_R}} \sum_{m=1}^{n_R} Q\left(\frac{\mathrm{sgn}(\Re[x_m^{(q)}])\Re[\mathbf{h}_m^T \mathbf{C}\,\mathbf{x}^{(q)}]}{\sigma_n}\right), \tag{19.26}$$

where $Q(\ )$ is the standard Gaussian error function, $\mathscr{M}^{n_R} = 4^{n_R}$ is the number of equiprobable legitimate transmit symbol vectors $\mathbf{x}^{(q)}$ for QPSK signalling (19.11) and $x_m^{(q)}$ the mth element of $\mathbf{x}^{(q)}$, with $1 \le q \le \mathscr{M}^{n_R}$. Similarly, the average BER of the quadrature-phase component of $\mathbf{y}(k)$ can be shown to be [8]

$$P_{e_Q}(\mathbf{C}) = \frac{1}{n_R \mathscr{M}^{n_R}} \sum_{q=1}^{\mathscr{M}^{n_R}} \sum_{k=1}^{n_R} Q\left(\frac{\mathrm{sgn}(\Im[x_m^{(q)}])\Im[\mathbf{h}_m^T \mathbf{C}\,\mathbf{x}^{(q)}]}{\sigma_n}\right). \tag{19.27}$$

Thus the average BER of the MUT with the precoder matrix $\mathbf{C}$ is given by

$$P_e(\mathbf{C}) = \big(P_{e_I}(\mathbf{C}) + P_{e_Q}(\mathbf{C})\big)/2, \tag{19.28}$$

Table 19.1 Computational complexity per iteration of two MBER MUT designs for QPSK signalling, where n_T is the number of transmit antennas, n_R the number of mobile terminals, $\mathscr{M} = 4$ is the size of symbol constellation and S is the swarm size

Algorithm	Flops
SQP	$n_R \times (8 \times n_T^2 \times n_R^2 + 6 \times n_T \times n_R + 6 \times n_T + 8 \times n_R + 4) \times \mathscr{M}^{n_R}$ $+\mathscr{O}(8 \times n_T^3 \times n_R^3) + 8 \times n_T^2 \times n_R^2 + 16 \times n_T \times n_R^2 + 8 \times n_T^2 \times n_R$ $+12 \times n_T \times n_R + 6 \times n_R^2 - 2 \times n_T^2 + n_T - 2 \times n_R + 11$
PSO	$((16 \times n_T \times n_R + 7 \times n_R + 6 \times n_T + 1) \times \mathscr{M}^{n_R} + 20 \times n_T \times n_R + 2) \times S + 8$

and the solution of the average MBER MUT is defined as

$$\mathbf{C}_{\text{TxMBER}} = \arg\min_{\mathbf{C}} P_e(\mathbf{C}) \quad \text{s.t. } E[\|\mathbf{C}\mathbf{x}(k)\|^2] = \mathrm{E_T}. \tag{19.29}$$

The optimisation problem (19.29) is a constrained nonlinear optimisation problems, and it is typically solved by an iterative gradient based optimisation algorithm known as the SQP [21, 23, 39]. The computational complexity per iteration of the SQP-based MBER MUT, quoted from [39], is listed in Table 19.1 for QPSK modulation, where $\mathscr{O}(8 \times n_T^3 \times n_R^3)$ stands for order of $8 \times n_T^3 \times n_R^3$ complexity and we assume that the complexity of a real-valued multiplication is equal to a real-valued addition. Note that $\mathscr{O}(8 \times n_T^3 \times n_R^3)$ is the complexity for matrix inversion required by the SQP algorithm, and the exact value of $\mathscr{O}(8 \times n_T^3 \times n_R^3)$ depends on the inversion algorithm employed. The total computational complexity equals the number of iterations that the algorithm required to arrive at a global optimal solution multiplied by this complexity per iteration.

19.4.3 PSO Aided MBER MUT Design

In practice, the computational complexity of the SQP based MBER-MUT solution may be excessively high for high-rate systems [23]. In this contribution, we invoke the PSO algorithm to solve the MBER-MUT design (19.29) in order to bring down the computational complexity to a practically acceptable level. A penalty function approach is adopted to convert the constrained optimisation process (19.29) into the unconstrained one and to automatically perform power allocation in order to meet the transmit power constraint. Let us define the cost function for the PSO algorithm to minimise as

$$F(\mathbf{C}) = P_e(\mathbf{C}) + G(\mathbf{C}) \tag{19.30}$$

with the penalty function given by

$$G(\mathbf{C}) = \begin{cases} 0, & E[\|\mathbf{C}\mathbf{x}(k)\|^2] - \mathrm{E_T} \le 0, \\ \lambda(E[\|\mathbf{C}\mathbf{x}(k)\|^2] - \mathrm{E_T}), & E[\|\mathbf{C}\mathbf{x}(k)\|^2] - \mathrm{E_T} > 0. \end{cases} \tag{19.31}$$

With an appropriately chosen penalty factor λ, the MBER-MUT design (19.29) can be obtained as the solution of the following unconstrained optimisation

$$\mathbf{C}_{\text{TxMBER}} = \arg\min_{\mathbf{C}} F(\mathbf{C}). \tag{19.32}$$

The value of λ is linked to the value of SNR. Since the BS has the knowledge of the downlink SNR, it is not difficult at all to assign an appropriate λ value. The dimensions of the search space for the PSO optimisation are specified by $N = n_T$ and $M = n_R$.

In Step *a) The swarm initialisation*, we set $\mathbf{C}_1^{(0)} = \mathbf{C}_{\text{TxMMSE}}$, the MMSE MUT solution, and randomly generate the rest of the initial particles, $\{\mathbf{C}_i^{(0)}\}_{i=2}^{S}$, in the search space $\mathsf{U}^{n_T \times n_R}$.

In Step *c) The swarm update*, we adopt the zero inertia weight $\xi = 0$ and the TVAC mechanism (19.8). If a particle wanders outside the search space, we move it back inside the search space randomly rather than forcing it to stay at the border of the search space. These measures are tested empirically to be appropriate for this application.

The computational complexity per iteration for the PSO-aided MBER-MUT scheme is also listed in Table 19.1. We will demonstrate that the PSO-aided MBER MUT design imposes a considerably lower complexity than the SQP based MBER MUT design. This is owing to the fact that the designed PSO algorithm is very efficient in searching through the precoder's parameter space to find an optimal solution, as demonstrated in the following simulation study.

19.4.4 Simulation Study

We considered the downlink of a multiuser system that employed $n_T = 4$ transmit antennas at the BS to communicate over the 4×4 flat Rayleigh fading MIMO channels to $n_R = 4$ single-receive-antenna QPSK MTs. The size of the swarm was chosen to be $S = 20$, and the corresponding maximum number of iterations for the PSO algorithm to arrive at the MBER performance was in the range of $I_{\max} = 20$ to 40, depending on the value of the downlink SNR. The choice of $S = 20$ was appropriate in this application as it led to the lowest computational cost for the algorithm to converge. Our empirical results suggested that the search limit $U_{\max} = 1.0$ and the velocity bound $V_{\max} = 1.0$ were appropriate for this application. The control factor γ in avoiding zero velocity was found to be $\gamma = 0.1$ by experiments. All the simulation results were obtained by averaging over 100 different channel realisations.

We first assumed the perfect channel state information (CSI) at the BS. Fig. 19.6 compares the BER performance of the MMSE-MUT scheme with that of the PSO-based MBER-MUT scheme. It can be seen from Fig. 19.6 that, given the perfect CSI, the PSO-aided MBER-MUT provided an SNR gain of 3 dB over the MMSE-MUT scheme at the target BER level of 10^{-4}. The robustness of the PSO-aided MBER-MUT design to channel estimation error was next investigated by adding a complex-valued Gaussian white noise with a standard deviation of 0.05 per

dimension to each channel tap $h_{i,m}$ to represent channel estimation error. The BERs of the MMSE-MUT and the PSO-based MBER-MUT under this channel estimation error are also plotted in Fig. 19.6. It can be seen that the PSO-aided MBER-MUT design was no more sensitive to channel estimation error than the MMSE-MUT design. The convergence performance and computational requirements of the PSO-aided MBER-MUT design were investigated, using the SQP-based MBER-MUT counterpart as the benchmark. Fig. 19.7 compares the convergence performance of the SQP-based and PSO-aided MBER MUT schemes, operating at the SNR values of $\mathrm{E_b/N_o} = 10$ dB and 15 dB, respectively.

At the SNR of 10 dB, it can be seen from Fig. 19.7 that the SQP algorithm converged to the MBER-MUT solution after 100 iterations, while the PSO counterpart arrived at the same MBER-MUT solution after 20 iterations. Fig. 19.8 shows the computational complexities required by the SQP-based and PSO-aided MBER-MUT designs, respectively, to arrive at the MBER MUT solution, in term of (a) the total number of operations (Flops) and (b) the total run time (seconds) recorded. In deriving the number of operations required by the SQP algorithm, we had approximated $\mathscr{O}(8 \times n_T^3 \times n_R^3)$ by $8 \times n_T^3 \times n_R^3$. It can be observed from Fig. 19.8 (a) that the SQP-based algorithm needed 229,351,100 Flops to converge to the MBER-MUT solution, while the PSO-aided algorithm converged to the same MBER-MUT solution at the cost of 34,561,760 Flops. Therefore, the PSO-aided MBER-MUT design imposed an approximately seven times lower complexity than the SQP counterpart

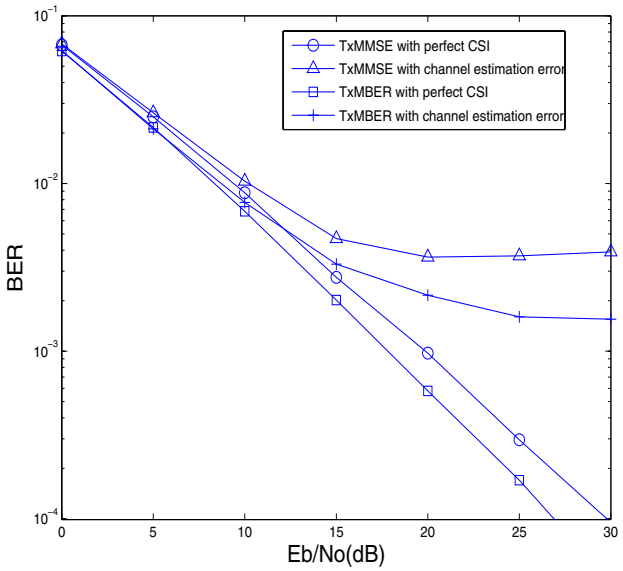

Fig. 19.6 BER versus SNR performance of the PSO-aided MBER-MUT communicating over flat Rayleigh fading channels using $n_T = 4$ transmit antennas to support $n_R = 4$ QPSK MTs, in comparison with the benchmark MMSE-MUT

for this scenario. From Fig. 19.8 (b), it can be seen that the SQP-based design required 1730.6 seconds to converge to the optimal MBER-MUT solution, while the PSO-aided design only needed 257.3 seconds to arrive at the same optimal MBER-MUT solution. This also confirms that the PSO-aided MBER-MUT scheme was approximately seven times faster than the SQP-based counterpart in this case.

From Fig. 19.7 it can also been that, with the SNR of 15 dB, the SQP based algorithm converged after 140 iterations, which required a total cost of 321,091,540 Flops, while the PSO-aided scheme archived the convergence after 40 iterations, which required a total cost of 63,541,120 Flops. Thus, the PSO-aided design imposed an approximately five times lower complexity than the SQP counterpart in this scenario.

Further investigation showed that the convergence results obtained for SNR$<$ 10 dB were similar to the case of SNR$=$ 10 dB, while the convergence results obtained under SNR$>$ 15 dB agreed with the case of SNR$=$ 15 dB. Thus, we may conclude that for this 4×4 MIMO benchmark the PSO-aided MBER-MUT design imposed approximately five to seven times lower complexity than the SQP-based MBER-MUT counterpart.

Finally, we showed that why the choice of the swarm size $S = 20$ was optimal in this application. Fig. 19.9 illustrates the convergence performance and the total required complexity for the PSO-aided algorithm with the different swarm sizes of $S = 10$, 20, 30 and 40 at the SNR value of 15 dB. It is clear that $S = 10$ was too small

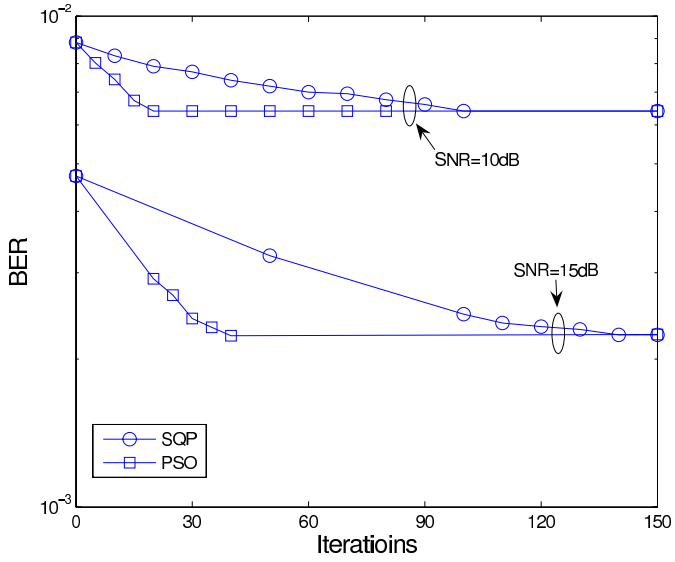

Fig. 19.7 Convergence performance of the SQP-based and PSO-aided MBER-MUT schemes for the system employing $n_T = 4$ transmit antennas to support $n_R = 4$ QPSK MTs over flat Rayleigh fading channels at $\mathrm{E_b}/\mathbf{N_o} = 10$ dB and 15 dB, respectively

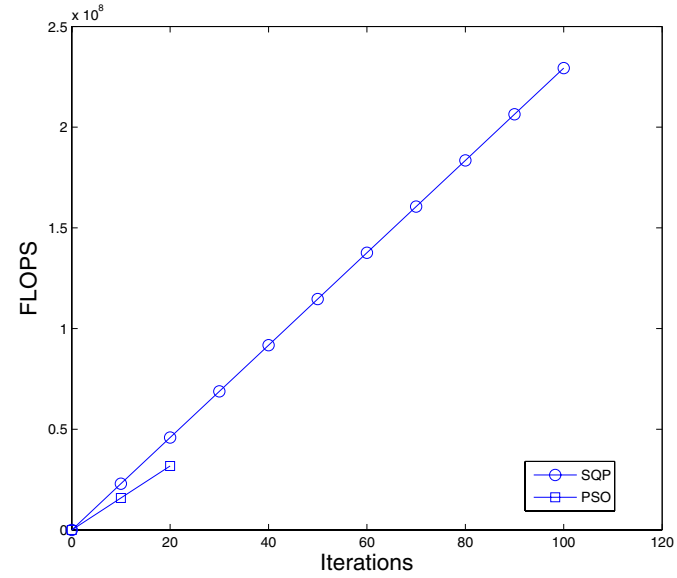

(a)

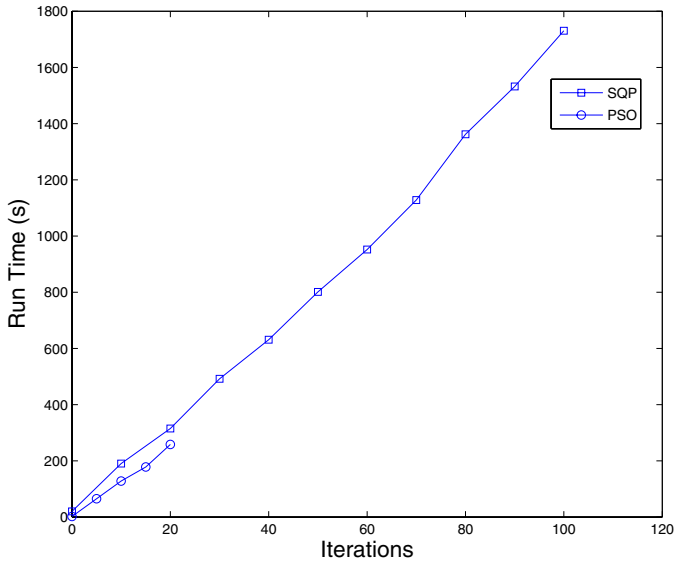

(b)

Fig. 19.8 Complexity comparison of the SQP-based and PSO-aided MBER-MUT schemes for the system employing $n_T = 4$ transmit antennas to support $n_R = 4$ QPSK MTs over flat Rayleigh fading channels at $\mathrm{E_b}/\mathbf{N_o} = 10$ dB, in terms of (a) number of FLOPs, and (b) run time (seconds)

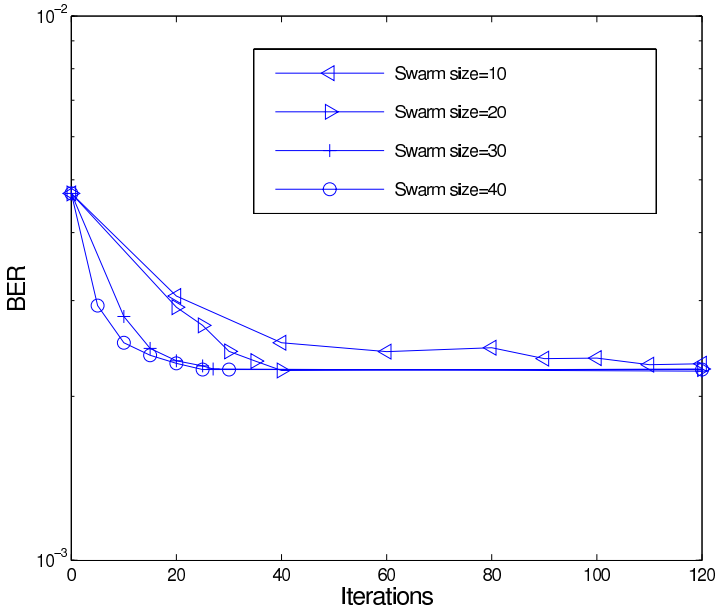

(a)

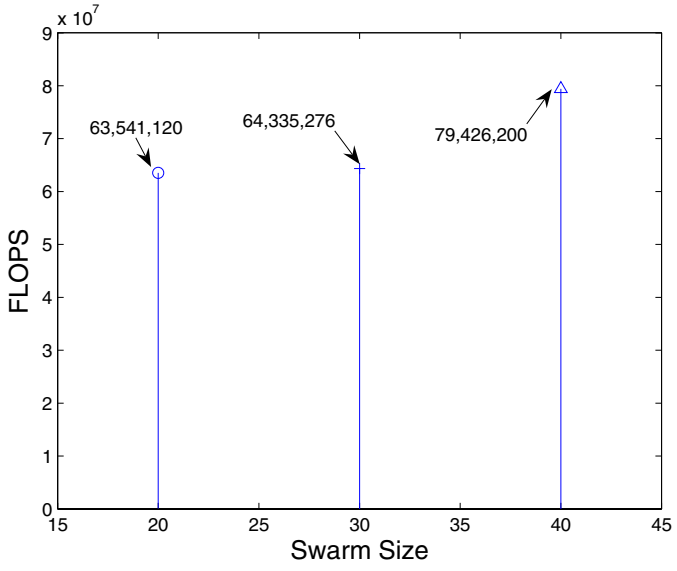

(b)

Fig. 19.9 Convergence performance (a) and required total complexity (b) of the PSO-aided MBER-MUT scheme with different swarm sizes for the system employing $n_T = 4$ transmit antennas to support $n_R = 4$ QPSK MTs over flat Rayleigh fading channels at $\mathrm{E_b}/\mathbf{N}_\mathrm{o} = 15$ dB

for the algorithm to converge to the optimal MBER-MUT solution in this case. The results of Fig. 19.9 also show that with $S = 20$ the algorithm took 40 iterations to converge at the cost of 63,541,120 Flops, and with $S = 30$ it needed 27 iterations at the cost of 64,335,276 Flops, while the algorithm given $S = 40$ only required 25 iterations to converge but its cost was 79,426,200 Flops. Thus the choice of $S = 20$ led to the lowest computational cost for the algorithm to converge in this application.

19.5 Conclusions

State-of-the-art MIMO transceiver designs impose expensive optimisation problems, which require the applications of sophisticated and advanced optimisation techniques, such as evolutionary computation methods, in order to achieve the optimal performance offered by MIMO technologies at practically affordable cost. In this contribution, we have demonstrated that the PSO provides an efficient tool for aiding MIMO transceiver designs. Specifically, we have applied the PSO algorithm to the semi-blind joint ML channel estimation and data detection for MIMO receiver, which offers significant complexity saving over an existing state-of-the-art RWBS-based scheme. Furthermore, we have employed the PSO to design the MBER MUT scheme for the downlink of a SDMA induced MIMO system, which imposes much lower computational complexity than the available SQP-based MBER MUT design.

The Communication Research Group at the University of Southampton has actively engaged in research of state-of-the-art MIMO transceiver designs using various powerful evolutionary computation methods for a long time. In particular, we have extensive experience using the genetic algorithm [3, 5, 6, 22, 24, 53] and the ant colony optimisation [47, 48, 49] for MUD designs. Further research is warranted to further investigate various evolutionary computation methods in benchmark MIMO designs and to study their performance-complexity trade-offs with the aim of providing useful guidelines for aiding practical MIMO system designs.

References

1. Abuthinien, M., Chen, S., Hanzo, L.: Semi-blind joint maximum likelihood channel estimation and data detection for MIMO systems. IEEE Signal Processing Letters 15, 202–205 (2008)
2. Akhtman, J., Wolfgang, A., Chen, S., Hanzo, L.: An optimized-hierarchy-aided approximate Log-MAP detector for MIMO systems. IEEE Trans. Wireless Communications 6(5), 1900–1909 (2007)
3. Alias, M.Y., Chen, S., Hanzo, L.: Multiple antenna aided OFDM employing genetic algorithm assisted minimum bit error rate multiuser detection. IEEE Trans. Vehicular Technology 54(5), 1713–1721 (2005)
4. Biguesh, M., Gershman, A.B.: Training-based MIMO channel estimation: A study of estimator tradeoffs and optimal training signals. IEEE Trans. Signal Processing 54(3), 884–893 (2006)

5. Chen, S., Wu, Y., McLaughlin, S.: Genetic algorithm optimisation for blind channel identification with higher-order cumulant fitting. IEEE Trans. Evolutionary Computation 1(4), 259–266 (1997)
6. Chen, S., Wu, Y.: Maximum likelihood joint channel and data estimation using genetic algorithms. IEEE Trans. Signal Processing 46(5), 1469–1473 (1998)
7. Chen, S., Wang, X.X., Harris, C.J.: Experiments with repeating weighted boosting search for optimization in signal processing applications. IEEE Trans. System, Man and Cybernetics, Part B 35(4), 682–693 (2005)
8. Chen, S., Hanzo, L., Ahmad, N.N., Wolfgang, A.: Adaptive minimum bit error rate beamforming assisted receiver for QPSK wireless communication. Digital Signal Processing 15(6), 545–567 (2005)
9. Chen, S., Livingstone, A., Du, H.-Q., Hanzo, L.: Adaptive minimum symbol error rate beamforming assisted detection for quadrature amplitude modulation. IEEE Trans. Wireless Communications 7(4), 1140–1145 (2008)
10. Das, S., Konar, A.: A swarm intelligence approach to the synthesis of two-dimensional IIR filters. Engineering Applications of Artificial Intelligence 20(8), 1086–1096 (2007)
11. El-Mora, H.H., Sheikh, A.U., Zerguine, A.: Application of particle swarm optimization algorithm to multiuser detection in CDMA. In: Proc. 16th IEEE Int. Symp. Personal, Indoor and Mobile Radio Communications, Berlin, Germany, September 11-14, vol. 4, pp. 2522–2526 (2005)
12. Fang, W., Sun, J., Xu, W.-B.: Design IIR digital filters using quantum-behaved particle swarm optimization. In: Proc. 2nd Int. Conf. Natural Computation, Part II, Xian, China, September 24-28, pp. 637–640 (2006)
13. Feng, H.-M.: Self-generation RBFNs using evolutional PSO learning. Neurocomputing 70(1-3), 41–251 (2006)
14. Foschini, G.J.: Layered space-time architecture for wireless communication in a fading environment when using multiple antennas. Bell Labs Tech. J. 1(2), 41–59 (1996)
15. Foschini, G.J., Gans, M.J.: On limits of wireless communications in a fading environment when using multiple antennas. Wireless Personal Communications 6(3), 311–335 (1998)
16. Guerra, F.A., Coelho, L.S.: Multi-step ahead nonlinear identification of Lorenz's chaotic system using radial basis function neural network with learning by clustering and particle swarm optimiszation. Chaos, Solitons and Fractals 35(5), 967–979 (2008)
17. Guo, Z., Xiao, Y., Lee, M.H.: Multiuser detection based on particle swarm optimization algorithm over multipath fading channels. IEICE Trans. Communications E90-B(2), 421–424 (2007)
18. Guru, S.M., Halgamuge, S.K., Fernando, S.: Particle swarm optimisers for cluster formation in wireless sensor networks. In: Proc. 2005 Int. Conf. Intelligent Sensors, Sensor Networks and Information Processing, Melbourne, Australia, December 5-8, pp. 319–324 (2005)
19. Hanzo, L., Münster, M., Choi, B.J., Keller, T.: OFDM and MC-CDMA for Broadband Multi-User Communications, WLANs and Broadcasting. John Wiley and IEEE Press, Chichester (2003)
20. Hanzo, L., Ng, S.X., Keller, T., Webb, W.: Quadrature Amplitude Modulation: From Basics to Adaptive Trellis-Coded, Turbo-Equalised and Space-Time Coded OFDM, CDMA and MC-CDMA Systems. John Wiley and IEEE Press, Chichester (2004)
21. Hjørungnes, A., Diniz, P.S.R.: Minimum BER prefilter transform for communications systems with binary signaling and known FIR MIMO channel. IEEE Signal Processing Letters 12(3), 234–237 (2005)

22. Hua, W.: Interference Suprression in Single- and Multi-Carrier CDMA Systems. PhD Thesis, School of Electronics and Computer Science, University of Southampton, Southampton, UK (2005)
23. Irmer, R.: Multiuser Transmission in Code Division Multiple Access Mobile Communication Systems. PhD Thesis, Technique University of Dresden, Dresden, Germany (2005)
24. Jiang, M.: Hybrid Multi-user OFDM Uplink Systems Using Multiple Antennas. PhD Thesis, School of Electronics and Computer Science, University of Southampton, Southampton, UK (2005)
25. Kennedy, J., Eberhart, R.: Particle swarm optimization. In: Proc. 1995 IEEE Int. Conf. Neural Networks, Perth, Australia, November 27-December 1, vol. 4, pp. 1942–1948 (1995)
26. Kennedy, J., Eberhart, R.: Swarm Intelligence. Morgan Kaufmann, San Francisco (2001)
27. Leong, W.-F., Yen, G.G.: PSO-based multiobjective optimization with dynamic population size and adaptive local archives. IEEE Trans. Systems, Man and Cybernetics, Part B 38(5), 1270–1293 (2008)
28. Liu, H., Li, J.: A particle swarm optimization-based multiuser detection for receive-diversity-aided STBC systems. IEEE Signal Processing Letters 15, 29–32 (2008)
29. Lu, Z., Yan, S.: Multiuser detector based on particle swarm algorithm. In: Proc. 6th IEEE CAS Symp. Emerging Technologies: Frontiers of Mobile and Wireless Communication, Shanghai, China, May 31-June 2, vol. 2, pp. 783–786 (2004)
30. Marzetta, T.L., Hochwald, B.M.: Capacity of a mobile multiple-antenna communication link in Rayleigh flat fading. IEEE Trans. Information Theory 45(1), 139–157 (1999)
31. Nocedal, J., Wright, S.J.: Numerical Optimization. Springer, New York (1999)
32. Paulraj, A., Nabar, R., Gore, D.: Introduction to Space-Time Wireless Communications. Cambridge University Press, Cambridge (2003)
33. Paulraj, A.J., Gore, D.A., Nabar, R.U., Bölcskei, H.: An overview of MIMO communications – A key to gigabit wireless. Proc. IEEE 92(2), 198–218 (2004)
34. Pham, D., Pattipati, K.R., Willet, P.K., Luo, J.: An improved complex sphere decoder for V-BLAST systems. IEEE Signal Processing Letters 11(9), 748–751 (2004)
35. Ratnaweera, A., Halgamuge, S.K., Watson, H.C.: Self-organizing hierarchical particle swarm optimizer with time-varying acceleration coefficients. IEEE Trans. Evolutionary Computation 8(3), 240–255 (2004)
36. Soo, K.K., Siu, Y.M., Chan, W.S., Yang, L., Chen, R.S.: Particle-swarm-optimization-based multiuser detector for CDMA communications. IEEE Trans. Vehicular Technology 56(5), 3006–3013 (2007)
37. Sun, J., Xu, W.-B., Liu, J.: Training RBF neural network via quantum-behaved particle swarm optimization. In: King, I., Wang, J., Chan, L.-W., Wang, D. (eds.) ICONIP 2006. LNCS, vol. 4233, pp. 1156–1163. Springer, Heidelberg (2006)
38. Sun, T.-Y., Liu, C.-C., Tsai, T.-Y., Hsieh, S.-T.: Adequate determination of a band of wavelet threshold for noise cancellation using particle swarm optimization. In: Proc. CEC 2008, Hong Kong, China, June 1-6, pp. 1168–1175 (2008)
39. Tan, S.: Minimum Error Rate Beamforming Transceivers. PhD Thesis, School of Electronics and Computer Science, University of Southampton, Southampton, UK (2008)
40. Tang, L., Liu, R.W., Soon, V.C., Huang, Y.F.: Indeterminacy and identifiability of blind identification. IEEE Trans. Circuits and Systems 38(5), 499–509 (1991)
41. Telatar, I.E.: Capacity of multi-antenna Gaussian channels. European Trans. Telecommunications 10(6), 585–595 (1999)

42. Tse, D., Viswanath, P.: Fundamentals of Wireless Communication. Cambridge University Press, Cambridge (2005)
43. Vandenameele, P., van Der Perre, L., Engels, M.: Space Division Multiple Access for Wireless Local Area Networks. Kluwer, Boston (2001)
44. Vojčić, B.R., Jang, W.M.: Transmitter precoding in synchronous multiuser communications. IEEE Trans. Communications 46(10), 1346–1355 (1998)
45. Winters, J.H.: Smart antennas for wireless systems. IEEE Personal Communications 5(1), 23–27 (1998)
46. Wolfgang, A.: Single-Carrier Time-Domain Space-Time Equalization Algorithms for the SDMA Uplink. PhD Thesis, School of Electronics and Computer Science, University of Southampton, Southampton, UK (2007)
47. Xu, C., Yang, L.-L., Hanzo, L.: Ant-colony-based multiuser detection for MC DS-CDMA systems. In: Proc. VTC 2007-Fall, Baltimore, USA, September 30-October 2, pp. 960–964 (2007)
48. Xu, C., Yang, L.-L., Maunder, R.G., Hanzo, L.: Near-optimum soft-output ant-colony-optimization based multiuser detection for the DS-CDMA. In: Proc. ICC 2008, Beijing, China, pp. 795–799 (2008)
49. Xu, C., Hu, B., Yang, L.-L., Hanzo, L.: Ant-colony-based multiuser detection for multi-functional antenna array assisted MC DS-CDMA systems. IEEE Trans. Vehicular Technology 57(1), 658–663 (2008)
50. Yang, L.-L.: Design of linear multiuser transmitters from linear multiuser receivers. In: Proc. ICC 2007, Glasgow, UK, June 24-28, pp. 5258–5263 (2007)
51. Yang, D., Yang, L.-L., Hanzo, L.: Performance of SDMA systems using transmitter preprocessing based on noisy feedback of vector-quantized channel impulse responses. In: In: Proc. VTC2007-Spring, Dublin, Ireland, pp. 2119–2123 (2007)
52. Yao, W., Chen, S., Tan, S., Hanzo, L.: Particle swarm optimisation aided minimum bit error rate multiuser transmission. In: Proc. ICC 2009, Dresden, Germany, 5 pages (2009)
53. Yen, K.: Genetic Algorithm Assisted CDMA Multiuser Detection. PhD Thesis, School of Electronics and Computer Science, University of Southampton, Southampton, UK (2001)